XRD-Rietveld Quantitative Analysis of Glass-containing By-products used in the Brazilian Cement Industry

L.A. Gobbo[1,2], L.M. Sant'Agostino[1], L.Z. D'Agostino[3]
[1]*Instituto de Geociências - Universidade de São Paulo, Brazil*
[2]*Panalytical, São Paulo, Brazil*
[3]*Laboratório de Caracterização Tecnológica, Escola Politécnica da Universidade de São Paulo, Brazil*

Abstract: This study was performed with samples of Brazilian industrial by-products: thermal stations fly ashes from the South region, iron metallurgy blast-furnace slags from the Southeast region, microsilica from the production of metallic silicon in the North region and rice husk ashes from the Central region. These materials contain amorphous phases, which are reactive when used as additions in Portland cement production. X-ray fluorescence (XRF), X-ray diffraction (XRD) and electron microscopy (SEM-EDS) were used to perform the study. XRD was performed using known quantities of lithium fluoride (LiF) and rutile (TiO_2) as internal standards. The Rietveld refinement method was applied to the XRD scans for quantitative analysis of amorphous and also crystalline phases. The comparison of these quantitative results showed the Rietveld Method to be a useful tool for qualification of the industrial by-products used in the cement industry.

1. Introduction

The aim of this research was to quantify some Brazilian cement additives containing glass, using the XRD Rietveld refinement method.
Yamamoto et al [1] classified cement-blending materials into industry byproducts and mineral deposits. The natural pozzolans come from mineral deposits mainly represented by analcimite, metakaolinite, tuff, diatomaceous earth, opaline shale, and tripoli, as reported by Massaza [2]. Alternatively artificial pozzolans originate from the treatment of natural materials.
The blastfurnace slag is usually characterized by a glass weight percent higher than 95. Glass content and mineral phases are controlled by chemical composition and quenching process parameters. The crystalline phases are generally merwinite, of mean composition $Ca_3MgSi_2O_8$ and melilite, a solid solution series between akermanite, $Ca_2MgSi_2O_7$, and gehlenite, $Ca_2Al_2SiO_7$. Other minerals that may occur are C_2S (α,α',β,γ), pseudowollastonite (CS), rankinite (C_3S_2), merwinite (C_3MS_2), monticellite

(CMS) and oldhamite (CaS). Minor components are anorthite (CAS), forsterite (M_2S), enstatite (MS), perovskite (CaO), TiO_2 and spinel (MA).
Alexandre and Sebileau [3] reported the chemical composition of French slag and Yamamoto et al [1] presented the chemical composition of the main Brazilian blastfurnace slags. The hydraulic property of the blastfurnace slags is mainly dependent on their chemical composition. Basic slags and those with a high degree of vitrification are more reactive. Cella et all [4] showed an XRD analysis procedure for the quantification of amorphous and crystalline phases using the RIR (Reference Intensity Ratio) - Rietveld method, using rutile as internal standard.
Using fly ash is a large environmental saving as each ton produced represents between 3 to 5 tons of intrinsic CO_2 emission, depending on coal specification [1]. Besides amorphous content the most common phases of fly ash are mullite, magnetite, hematite, gypsum and quartz. Chemical compositions of Brazilian fly ashes are presented by Kihara and Scandiuzzi [5]. Rietveld quantification of some North American fly ash standard reference materials (NIST) were performed using the rutile as internal standard and the refinement was obtained with the GSAS software [6]. Synthetic corundum and zinc oxide were also used as internal standards to estimate the glass content of some Australian fly ashes [7].
Microsilica and rice husk ash are highly reactive pozzolanic materials, due to the combination of two factors, their almost totally non-crystalline structure and high surface area [8]. Although they are comparable in performance characteristics in concrete, their chemical and physical properties show some essential differences.
Different techniques mostly used to study glassy materials are microscopy, chemical dissolution and mechanical analysis. XRD is another technique that can also be applied to study those materials. In the Rietveld method [9] a theoretical XRD pattern is calculated and fitted to an observed powder scan until the calculation describes the observed pattern as closely as possible. The calculation of a theoretical powder pattern requires crystal structure information about the phases present. The accuracy of the quantification is directly dependent on the quality of the structural and instrumental parameters. The Rietveld method is currently being used to determine the crystalline phase fractions in Portland cements. Overviews concerning the application of the Rietveld method to clinker analysis have been more recently given [10,11,12,13,14,15].
The quantification of amorphous phase is a step forward in the greater use of Rietveld quantitative analysis. Analyses of amorphous phases using internal standards as reported by De La Torre et al [16] show that Al_2O_3 gave the best results for several samples.

2. Methods

The following samples of Brazilian by-products were studied: power station fly ashes from the south region, iron metallurgy blast-furnace slags from the southeast region, microsilica from the production of metallic silicon in the north region and the rice husk ashes from the central region. X-ray fluorescence (XRF), X-ray diffraction (XRD) and electron microscopy (SEM-EDS) were used to perform the research. The research was performed at the Panalytical Application Laboratory associated with the Technological Characterization Laboratory from the Polytechnic School of the University of São Paulo.

2.1 X-Ray fluorescence (XRF)

Standardless chemical analyses were performed by X-ray fluorescence using a Panalytical Axios Advanced (4KW) instrument. The XRF samples were prepared as discs by fusing a mixture of the finely crushed sample with lithium tetraborate.

2.2 Optical microscopy

Transmitted optical light microscopy was used for point counting of 500 grains of each blastfurnace slags samples. It was also determined whether the refraction index of each sample was above or below 1,63. This classifies the samples as basic or acidic respectively.

2.3 Electron microscopy (SEM-EDS)

For electron microscopy analysis the samples were mounted in a double face carbon tape, coated by a platinum film and analyzed in an electron microscope (SEM) Stereoscan 440, Leo, with an energy dispersive x-ray spectrometer system (EDS), Oxford (Inca), with germanium detector.

2.4 X-Ray diffraction (XRD)

The first step for the XRD analysis was the selection of the best internal standard to be use in the quantification. Several internal standards were tested (Al_2O_3, CaF_2, Cr_2O_3, LiF, TiO_2, ZnO).
Lithium fluoride (LiF) was selected as the internal standard for the analysis of blastfurnace slags, fly ash and also microssílica, due to the presence of only three peaks, restricting the peak overlap. They came from a Brazilian producer (Dinâmica) and have 99.5% of LiF. Minor elements are Cl (0.005%), Fe (0.005%) and also SO_4 (0.05%). The granulometry analysis showed that 90% of the sample are below 23μm and 50% are below 10μm. Figure 1 shows an example of one pure fly ash sample and the same sample with 10% of the internal standard LiF. Initially rutile (TiO_2)

was also used, but some rutile was detected in 2 samples of fly ash limiting its application for this material. Rutile was used as an internal standard for the analysis of rice husk ash. The proportion of the internal standard was of 10% of the total mass.

X-ray powder diffraction analysis (XRD) was made using a Bragg-Brentano diffractometer (Panalytical X'Pert Pro) with a fine long focus CuKα anode tube operated at 40KV/40mA and a ½º divergence slit. The detector used was the X'Celerator, a multiple strip position sensitive detector that allows faster data collection than a traditional point detector.
The samples were mounted in a 27 mm diameter ring holder. The scans were made from 5 to 70 º2θ with a step size of 0.02 º2θ. Counting time from 30-60 seconds per point were used. The recorded X-ray diffractograms scans are available in computer files and can be loaded directly into Rietveld program for further analysis.
Cluster analysis (software from Panalytical - X'Pert HighScore Plus) was applied to the samples scans of blastfurnace slags. It is a multivariate analysis technique that seeks to organize information about variables so that relatively homogeneous groups, or "clusters", can be formed. This analysis was used to make groups of samples by similarity and to try to correlate those groups with the Rietveld results.
Structural data were selected after phase identification and were obtained from the ICDD data files (International Center for Diffraction Data).
Data sets were refined by the Rietveld method. The background was fitted with an available background function of the software. The peak profiles were modeled using a pseudo-Voight function. The lattice constants, the phase fraction, and zero shift were also refined. Preferred orientation was refined for some samples.

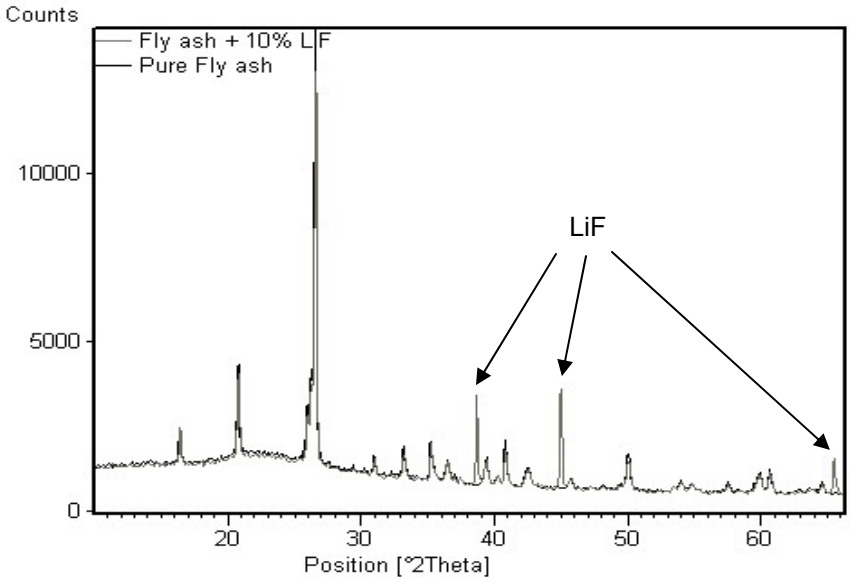

Figure 1: Fly ash sample with and without internal standard.

3. Results

3.1 Chemical composition

The chemical composition of blastfurnace slags, fly ashes, microsilica and rice husk ashes by XRF are presented in Table 1. All results were normalized to 100%.

Table 1: Chemical composition of blastfurnace slags (S); fly ashes (F); Microsilica (M); and Rice husk ash (R).

Sample	Na_2O	MgO	Al_2O_3	SiO_2	SO_3	K_2O	CaO	TiO_2	MnO	Fe_2O_3	LOI
S1	0.2	9.8	12.6	33.6	2.5	0.4	39.5	0.6	0.3	0.3	-
S2	0.2	10.0	12.3	33.8	2.5	0.4	39.2	0.7	0.3	0.4	-
S3	0.2	9.7	12.4	33.4	2.5	0.5	39.6	0.6	0.4	0.4	-
S4	0.2	9.8	12.6	33.7	2.4	0.4	38.9	0.7	0.4	0.4	0.2
S5	0.2	10.0	12.7	33.9	2.6	0.4	38.5	0.6	0.3	0.4	0.1
S6	0.2	10.2	12.6	34.3	2.6	0.4	37.7	0.6	0.3	0.5	0.3
S7	0.2	7.3	11.6	33.1	2.2	0.5	40.1	3.2	0.5	0.8	0.3
S8	0.2	7.3	11.5	33.7	2.6	0.4	41.1	2.2	0.4	0.3	-
S9	0.2	6.9	11.1	33.3	2.6	0.4	42.4	2.0	0.4	0.4	-
S10	0.2	7.6	10.3	34.2	2.3	0.4	43.0	0.7	0.6	0.4	-
S11	0.3	1.6	9.0	43.6	0.5	2.7	37.2	0.5	0.1	4.0	-
S12	0.3	1.5	9.2	43.6	0.3	3.2	37.4	0.7	0.1	3.1	-
S13	0.2	1.6	9.2	46.2	0.4	3.8	32.2	0.7	0.2	2.5	2.6
S14	0.2	1.7	9.7	47.4	0.4	3.2	32.5	0.6	0.1	3.7	-
S15	0.2	1.6	10.1	45.8	0.4	3.0	34.5	0.6	0.1	3.0	-
S16	0.2	1.9	8.6	43.6	0.3	2.6	26.3	0.5	0.5	15.0	-
S17	0.2	1.5	8.3	47.2	0.4	2.8	33.4	0.5	0.1	3.8	1.2
F2	0.2	0.4	23.8	65.1	0.3	1.3	3.0	1.4	0.0	4.3	-
F4	0.2	0.4	26.6	63.0	0.5	1.3	2.4	1.5	0.0	3.9	-
F6	0.4	0.6	25.6	59.9	-	3.1	1.3	1.8	0.0	6.8	-
F9	0.1	0.5	17.5	63.8	0.2	1.5	3.7	1.1	0.1	11.1	-
F10	0.1	0.4	18.1	69.9	0.3	1.5	3.3	1.5	0.0	4.7	-
F12	0.2	0.6	19.2	70.6	0.2	2.0	0.9	1.1	0.0	4.9	-
M1	0.2	0.6	0.1	96.1	-	1.2	0.2	-	-	0.1	1.1
M2	0.2	0.5	0.1	95.5	-	0.8	0.2	-	-	0.4	1.9
M3	0.2	0.4	0.1	96.5	-	0.8	0.3	-	-	0.2	1.1
M4	0.2	0.7	0.1	96.8	-	0.6	0.2	-	-	0.0	1.0
R*	0.1	0.5	0.1	90.1	0.1	2.6	1.0	-	0.4	3.8	-

LOI=Loss on Ignition; (*)Average result of rice husk ashes; (-) below detection limits;

3.2 Microscopic results (blastfurnace slags)

The microscopic results obtained are presented in the Table 2. Refraction index (n), CaO/SiO_2 relation and also hydraulic index [17] are also presented. It was verified that the acid slags presented glass weight percentage from 43 to 76, and basic slags from 87 to 99.
Basic slags were considered those with CaO/SiO_2 with the refraction index higher than 1,63.

Table 2: Weight % of glass from slags by microscopy point counting.

Amostra	n	Basic/Ácid	wt% of glass (m)	CaO/SiO_2	HI* Germany	HI** Brazil
S1	>1.64	Basic	87.3	1.17	1.27	1.84
S2	>1.64	Basic	88.7	1.16	1.27	1.82
S3	>1.64	Basic	89.0	1.19	1.28	1.85
S4	>1.64	Basic	90.1	1.15	1.26	1.82
S5	>1.64	Basic	90.2	1.14	1.25	1.81
S6	>1.64	Basic	90.8	1.10	1.22	1.77
S7	>1.64	Basic	93.9	1.21	1.25	1.78
S8	>1.64	Basic	99.2	1.22	1.26	1.77
S9	>1.64	Basic	99.2	1.28	1.30	1.82
S10	>1.64	Basic	94.9	1.26	1.32	1.78
S11	<1.62	Acid	62.1	0.85	0.84	1.09
S12	<1.62	Acid	69.4	0.86	0.84	1.10
S13	<1.62	Acid	70.4	0.70	0.70	0.93
S14	<1.62	Acid	53.3	0.69	0.69	0.93
S15	<1.62	Acid	76.3	0.75	0.75	1.01
S16	<1.62	Acid	61.8	0.60	0.63	0.84
S17	<1.62	Acid	43.7	0.71	0.71	0.91

n=refraction index;(m)=microscopy; HI-Hydraulic Index. (*)$HI=[CaO+MgO+(⅓Al_2O_3)]/[SiO_2+(2/3xAl_2O_3)]$; (**)$HI=(CaO+MgO+Al_2O_3)/SiO_2$

3.3 SEM

Some SEM images with their descriptions are presented in the Figure 2.

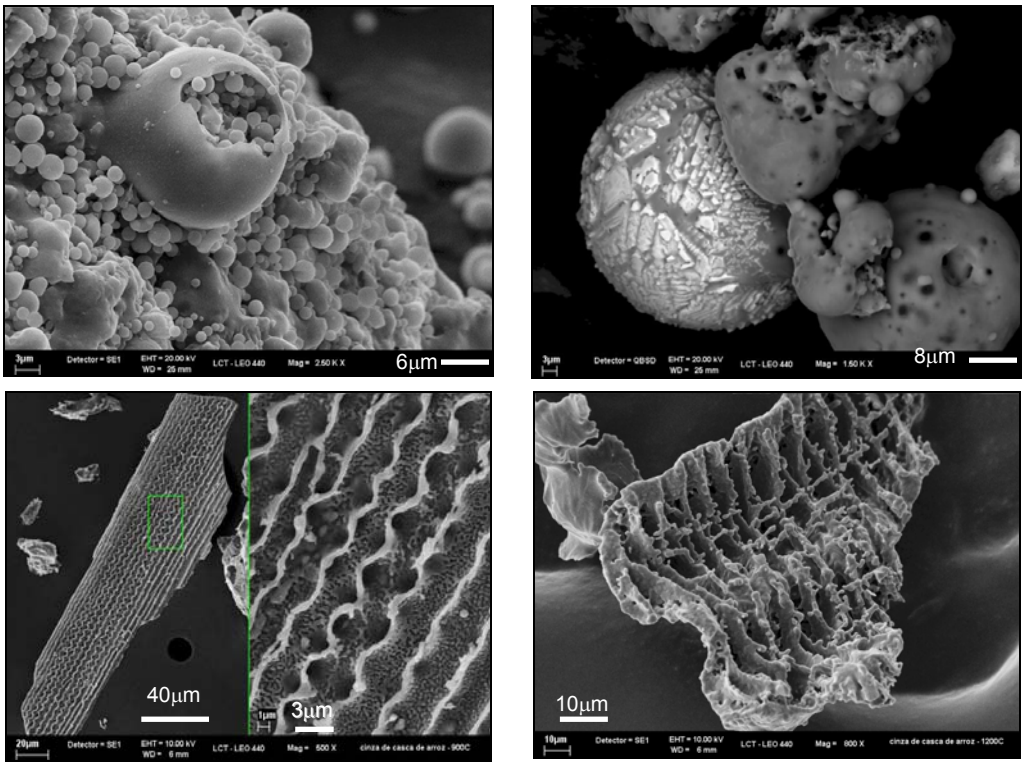

Figure 2: SEM images of (a) F6 - plerosphere with cenospherical particles; (b) F8– backscattering image of bottom ash plerosphere covered by Fe enriched crystals; (c)R1–rice husk ash burned at 900°C; (d) R2–rice husk ash burned at 1.200°C showing the skeletal aspect and high specific area.

3.4 XRD

Cluster analysis was initially applied to the more representative group of samples: blastfurnace slag. With this tool was possible to make groups of samples by scans similarity. Dendrogram was obtained by a hierarchic cluster and is presented in the Figure 3.

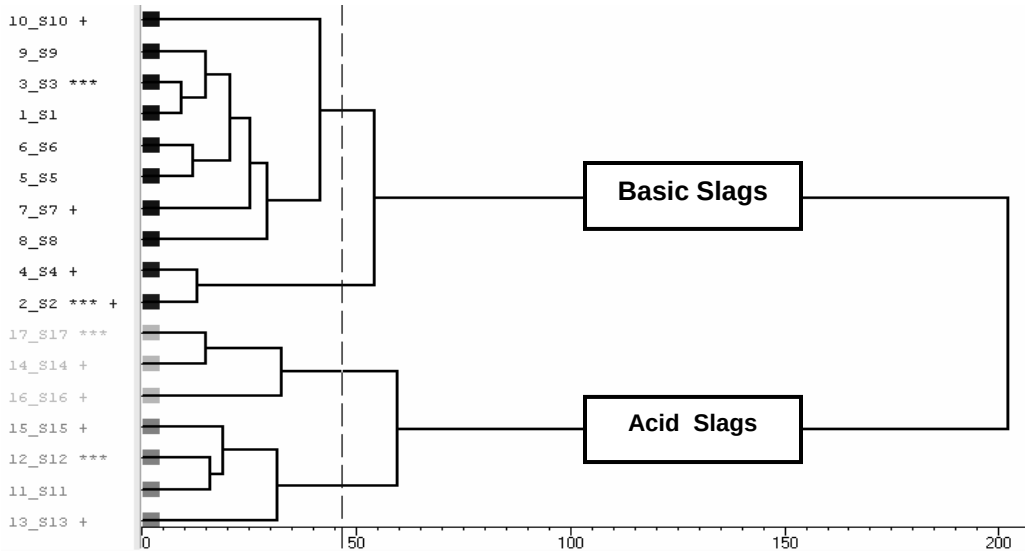

Figure 3: Dendrogram of the slag samples cluster analysis (sample versus cut-off).

It was used the Euclidian distance measure with the average linkage method for clustering. Using a manual cut-off, four clusters were obtained for the slags and also for the fly ashes samples.

One example of scans of each different analyzed material, with their Rietveld refinement graphics are shown in the Figure 4. The Figure 4a shows in three lines the position of the LiF peaks. The difference plot graphic shows the attained fitting of each refinement. GOF (goodness of fitting) of all analyzed samples were below 3,0.

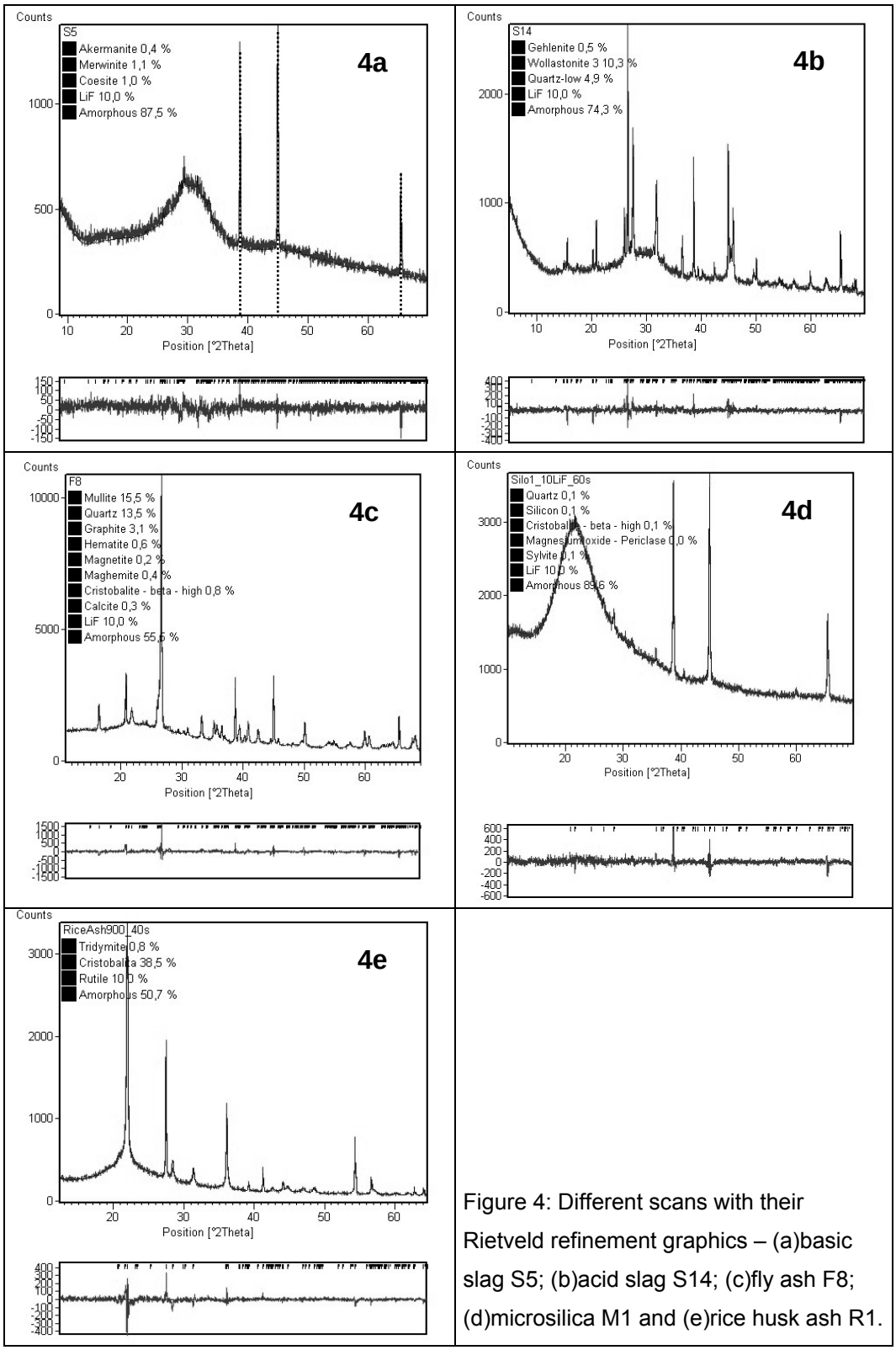

Figure 4: Different scans with their Rietveld refinement graphics – (a)basic slag S5; (b)acid slag S14; (c)fly ash F8; (d)microsilica M1 and (e)rice husk ash R1.

The Rietveld results were totalized considering the internal standard percentage of 10(%), and in the final quantitative results they were

discounted with the values redistributed to 100%, as shown in the Table 3 to 6.

Table 3: Phase composition of blastfurnace slags based on Rietveld method(wt%).

Sample	Phases (wt%) / ICSD code								
	Merwin. 43078	Gehlen. 87144	Akerm. 94146	Wollast. 201537	Quartz 73071	Coesite 100755	Anorth. 202712	Magh. 44517	Amorph
S1	0.7	-	-	-	-	2.2	-	-	97.1
S2	0.7	-	-	0.7	-	0.8	-	-	97.8
S3	1.4	-	0.7	-	-	0.9	-	-	97.0
S4	1.1	-	0.6	-	-	-	-	-	98.1
S5	1.2	-	0.4	-	-	1.1	-	-	97.2
S6	0.1	-		-	-	1.4	-	-	98.4
S7	0.7	-	0.6	-	-	-	-	-	98.7
S8	0.1	-	0.4	-	-	-	-	-	99.4
S9	-	-	0.4	-	-	0.6	-	-	99.0
S10	0.6	-	-	-	-	-	-	-	99.4
S11	-	1.0	1.6	-	3.9	-	2.7	0.6	90.4
S12	-	0.4	0.3	3.9	3.0	-	-	-	92.3
S13	0.3	0.4	-	7.0	5.8	-	-	-	86.3
S14	-	0.6	-	11.4	5.4	-	-	-	82.6
S15	-	1.0	0.2	2.9	6.8	-	-	-	89.1
S16	0.3	0.6	1.2	4.4	4.8	-	-	0.2	88.4
S17	-	2.0	-	13.3	8.3	-	-	-	76.1

Merw=Merwinite;Geh=Gehlenite;Aker=Akermanite;Wol=Wollastonite;Anort=Anorthoclase;Magh=Maghemite

Table 4: Phase composition of fly ash based on Rietveld method (wt%).

Sample	Phases (wt%) / ICSD code										
	Mulite 23867	Quartz 73071	Graph. 88810	Hem. 96076	Magn. 85807	Magh. 44517	Calcite 100676	Rutile 202240	Anat. 92363	Brook 88380	Amorph
F1	10.6	16.3	2.3	0.1	0.3	0.4	-	-	-	-	69.9
F2	21.3	15.9	2.3	0.1	-	0.2	0.2	-	-	-	59.7
F3	21.0	17.0	3.0	0.1	0.1	0.2	-	-	-	-	58.6
F4	23.9	23.0	3.1	0.1	-	-	-	-	-	-	49.9
F5	16.4	26.2	2.4	0.4	-	-	-	0.4	0.8	-	53.2
F6	22.9	11.2	2.7	0.2	0.1	0.2	-	-	-	-	62.7
F7	23.7	11.2	1.8	0.3	0.1	0.4	-	-	-	-	62.4
F8	17.2	15.0	3.4	0.7	0.2	0.4	0.3	-	-	0.9	61.7
F9	15.4	19.3	2.7	0.7	0.3	0.9	-	-	-	2.2	58.4
F10	15.0	18.0	2.2	0.1	-	0.3	0.4	-	-	-	63.9
F11	18.7	17.9	2.3	0.1	-	0.2	-	-	-	-	60.9
F12	15.6	22.1	3.1	0.1	-	0.2	-	-	-	-	58.9

Graph=Graphite;Hem=Hematite;Magn=Magnetite;Magh=Maghemite;Anat=Anatase;Brook=Brookite

Table 5: Phase composition of rice husk ash based on Rietveld method(wt%).

Sample	Phases (wt%) / ICSD code		
	Cristobalite-β 77462	Tridymite 413210	Amorphous
R1	42.8	0.9	56.3
R2	89.8	10.2	0.0

Table 6: Phase composition of microssílica based on Rietveld method (wt%).

Sample	Phases (wt%) / ICSD code				
	Quartz 73071	Silicon 60389	Cristobalite α 77456	Sylvite 61557	Amorphous
M1	0.1	0.1	0.1	0.1	99.6
M2	0.0	0.0	0.1	0.1	99.8
M3	0.2	0.0	0.1	0.1	99.6
M4	0.1	0.0	0.1	0.0	99.7

4. Discussion

Rietveld-based X-ray diffraction analysis provided a useful technique for glassy materials characterization, allowing the proportions of the different compounds and the glass within the samples to be evaluated in quantitative terms. As expected, microsilica was the material with higher content of glass.

The XRD-Rietveld results showed a good consistency in face of other quantitative technique used for the studied materials. The comparison of 17 blastfurnace slags samples results showed very good correlation for the amorphous (glassy) content by Rietveld method and microscopy point counting (R^2=0,91). Also a good accordance was found between the CaO/SiO_2 obtained by XRF and Rietveld glassy content results. When the ten basic slags are analyzed separately, it is possible to find a good correlation (R^2=0,74); and some correlation for the seven acid slags (R^2=0,70). The correlation graphics are shown in the Figure 5. The differences observed essentially in the lower limits of amorphous content samples are probably due to the subjectivity of the microscopic point counting analysis. Analysis of a larger number of samples would be required to better correlate the 2 different techniques.

The cluster analysis applied to the XRD scans was able to divide the slag samples in 2 bigger groups, one of acid slags and other of basic slags. Also this analysis was useful in the fly ashes types' classification (fly ash and bottom ash).

This research shows the Rietveld Method as an important tool for qualification and quantification of cement active additions from industrial byproducts.

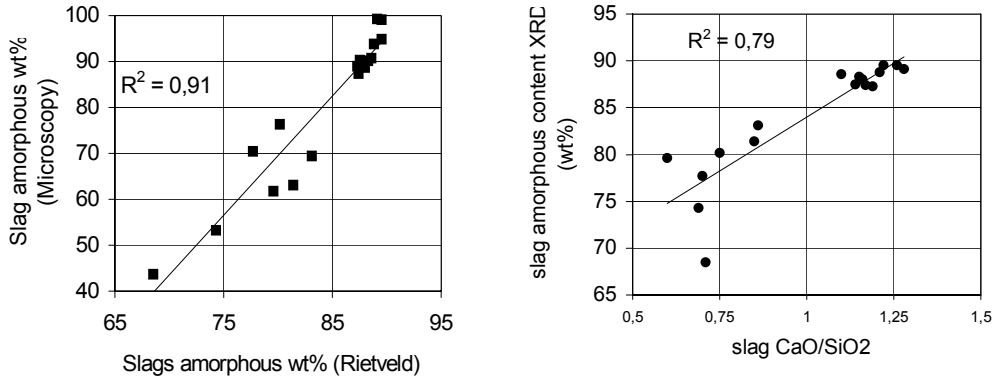

Figure 5: Correlations - slag glassy content versus point counting and CaO/SiO_2.

5. References

[1] J. K. Yamamoto, Y. Kihara, A. M. Coimbra, T. J. Montanheiro, , Environmental Impact Reduction on the Production of Blended Portland Cement in Brazil, Environmental Geosciences, 4, 192-206, 1997

[2] F. Massazza, Pozzolana and pozzolanic cements. In: LEA'S Chemistry of Cement and Concrete. Forth Edition. Peter C. Hewlett (ed.). Ed. Butterworth Heinemann. p. 471-636, 1998

[3] J. Alexandre, J.L.Sebileau, Le latier de haut founeau, C. T. P. L. ed., 1988

[4] Cella, F., Artioli, G., Gobbo, L. A., 1999, Characterization of blastfurnace slag used in composite cements by X-ray diffraction and fluorescence analysis, 5th Brazilian Conference on Portland Cement, 1-10.

[5] Kihara, Y., Scandiuzzi, L. 1992, Use of ash from coal combustion in the Brazilian cement industry. São Paulo, Brasil: Brazilian Portland Cement Association.

[6] Winburn, R. S., Grier, D. G., McCarthy, J., Peterson, R. B., 2000, Rietveld Quantitative X-ray diffraction analysis of NIST fly ash standard reference materials, Powder Diffraction, 15, 163-172.

[7] C. R. Ward, D. French, Determination of glass content and estimation of glass composition in fly ash using quantitative X-ray diffractometry, Fuel, Elsevier, 10, Article in press, 2006.

[8] V. M. Malhorta, P. K. Mehta, Pozzolanic and cementitious materials. Advances in Concrete Technology, V.1, 191, 1996.

[9] H. M. Rietveld, A profile refinement method for nuclear and magnetic structures, J. Appl. Crystallogr. 65-71, 1969

[10] M. A. G. de la Torre, Estudio de cementos y materials relacionados por el método de Rietveld. PhD Thesis. Universidad de Málaga, Spain, 2003

[11] J.Neubauer, H. Pöllmann, H.W. Meyer, Quantitative X-ray Analysis of OPC Clinker By Rietveld Refinement, International Congress on the Chemistry of Cement, 10 569-580, 1997

[12] H.W. Meyer, J. Neubauer, S. Malovrh., Neue Qualitätssicherung mit standard-freier Klinkerphasenbestimmung nach der Rietveld-Verfeinerung im Einsatz, ZKG International 3 152-162, 1998

[13] J.C. Taylor, I. Hinczak and C.E. Matulis, Rietveld full-profile quantification of Portland cement clinker: The importance of including a full crystallography of the major phase polymorphs, Powder Diffraction 15 (1), 7, 2000

[14] L. A. Gobbo, Os compostos do clínquer Portland: sua caracterização por difração de raios-X e quantificação poe refinamento de Rietveld. Master in Science Dissertation. University of Sao Paulo, Brazil, 2003

[15] L. A. Gobbo, L. M. Sant'Agostino, L. L. Garcez, Quantitative analysis of white cement clinker with Rietveld method., ICAM – International Congress of Applied Mineralogy, 2004

[16] A. G. De La Torre, S. Bruque, M. A. G. Aranda, Rietveld quantitative amorphous content analysis. Journal of Applied Crystallography, 34, 196-202, 2001.

[17] ABCP, Associação Brasileira de Cimento Portland, Contribuição ao conhecimento das propriedades do cimento Portland de alto forno (90), 111, 1988.